Optimality Analysis of Sensor-Target Geometries in Passive Localization: Part 1 - Bearing-Only Localization

Adrian N. Bishop [1], Barış Fidan [2], Brian D.O. Anderson [2], Kutluyıl Doğançay [3], Pubudu N. Pathirana [1]
[1] *School of Engineering and Information Technology, Deakin University, adrian.bishop@ieee.org*
[2] *Australian National University and National ICT Australia,* [3] *The University of South Australia*

Abstract

In this paper we characterize the relative sensor-target geometry for bearing-only localization in $\mathbb{R}^2$. We analyze the geometry in terms of the Cramer-Rao inequality and the corresponding Fisher information matrix, aiming to characterize and state explicit results in terms of the potential localization performance. In particular, a number of interesting results are rigorously derived which highlight erroneous assumptions often made in the existing literature.

1. Introduction

Currently the two most common passive measurement technologies available for localization and tracking are bearing measurements [1]–[4] and time-of-arrival based measurements (or time-difference-of-arrival measurements) [5]. However, in this paper we focus on bearing (or angle of arrival (AOA)) based localization systems in $\mathbb{R}^2$. This paper is part 1 of a pair of papers characterizing the relative sensor-target geometry in terms of the lower bounds on the potential localization accuracy. In part 2 [6] the relative sensor-target geometry for a time-of-arrival (or time-difference) based localization problem is characterized in a similar fashion.

It is well known that the relative sensor-target geometry plays a significant role in potential localization performance [1]. A number of papers [1], [7], [8] provide a partial characterization of the sensor-target geometry with various metrics (all related to the Cramer-Rao inequality). Indeed, the Cramer-Rao bound itself has played a role in determining optimal sensor trajectories and control laws for bearing-only localization and target tracking in numerous papers in the literature, e.g. see [1], [9]–[13] and the many references therein. In this paper we provide a more rigorous characterization of the relative sensor-target geometry for bearing-only localization that, to the best of the authors knowledge, cannot be found explicitly in the literature. We state specific results in terms of the relative angular geometry of the sensors with respect to the target. In particular, we look at the problem of finding the optimal angular configuration of sensors given arbitrary target ranges (and under some estimator assumptions).

The remainder of this paper is organized as follows. In Section 2 we outline some notation and conventions for bearing-only localization. In Section 3 we introduce the Cramer-Rao inequality and the related Fisher information matrix. Moreover, in Section 3 we discuss the relationship of the Fisher information matrix to geometric characterizations and we derive the Fisher information matrix and determinant for bearing-only localization with an arbitrary number of sensors. In Section 4 we explore the bearing-only localization geometry in detail and provide some informative illustrations. In Section 5 we give our conclusion.

The work of A.N. Bishop was supported by the Australian Research Council (ARC) and performed during a visit to National ICT Australia (NICTA) sponsored by NICTA. The work of K. Dogancay was supported by the Defence Science and Technology Organisation (DSTO). The work of B.D.O. Anderson and B. Fidan was supported by National ICT Australia. National ICT Australia is funded by the Australian Government's Department of Communications, Information Technology and the Arts and the Australian Research Council through the Backing Australia's Ability Initiative and the ICT Centre of Excellence Program. The work of P.N. Pathirana was supported by the Australian Research Council (ARC).

2. Notation and Related Conventions

We consider a single stationary target and multiple sensors all located in $\mathbb{R}^2$. The single target's location is given by $\mathbf{p} = [x_p \ y_p]^T$. Consider a number of sensors labeled $1, \ldots, N \geq 2$ with the location of the i^{th} sensor given by $\mathbf{s}_i = [x_{si} \ y_{si}]^T$. Let the range between the i^{th} sensor $\mathbf{s}_i$ and the target $\mathbf{p}$ be given by $r_i = \|\mathbf{p} - \mathbf{s}_i\|$. The angle subtended at the target by two sensors i and j is denoted by $\vartheta_{ij} = \vartheta_{ji} \in [0, \pi)$.

A. Bearing Conventions

The true azimuth bearing ϕ_i from sensor i to the target is measured clockwise from the global North direction and such that $\phi_i(\mathbf{p}) \in [0, 2\pi)$. The measured value of ϕ_i is given by $\widehat{\phi}_i = \phi_i(\mathbf{p}) + e_i$ where e_i is the measurement *error*. The e_i term is assumed to be normally distributed with zero mean and variance σ_ϕ^2, i.e. $e_i \sim \mathcal{N}(0, \sigma_\phi^2)$. It is common to mathematically model the bearing with the following equation

$$\phi_i(\mathbf{p}) = \arctan2\left(x_p - x_{si}, \ y_p - y_{si}\right) \tag{1}$$

where the $\arctan2$ function is defined such that $\phi_i(\mathbf{p}) \in [0, 2\pi)$ (note that $\arctan2$ is related to the standard $\arctan$ function and is common in many computer programming languages). The set of measurements from N sensors can be written as $\widehat{\mathbf{\Phi}} = \mathbf{\Phi}(\mathbf{p}) + \mathbf{e}$ where $\mathbf{\Phi}(\mathbf{p}) = [\phi_1(\mathbf{p}) \ \ldots \ \phi_N(\mathbf{p})]^T$

and $\mathbf{e} = [e_1 \ \dots \ e_N]^T$. We assume that the measurement errors of distinct sensors are mutually independent. Moreover, for simplicity, we assume that the error variances of multiple distinct sensors are equal and given by σ_ϕ^2. The covariance matrix of $\mathbf{e}$ is then given by $\mathbf{R}_\phi = \sigma_\phi^2 \mathbf{I}_N$ where $\mathbf{I}_N$ is an N-dimensional identity matrix. The general measurement vector $\widehat{\mathbf{\Phi}}$ can thus be considered an *observable* normally distributed random *vector* and can be described by $\widehat{\mathbf{\Phi}} \sim \mathcal{N}(\mathbf{\Phi}(\mathbf{p}), \mathbf{R}_\phi)$.

B. Comment on Relative Geometric Configurations

Without loss of generality we will always arrange the sensor indexing such that the true bearings obey $\phi_j \geq \phi_i$ when $j > i$ and $\forall i, j \in \{1, \dots, N\}$. Essentially we can always re-number the sensor locations or rotate the coordinate system such that this arrangement holds.

3. The Cramer-Rao Inequality and Fisher Information For Bearings Localization in $\mathbb{R}^2$

The Cramer-Rao bound states that under (two) mild regularity conditions the minimum variance achievable by an unbiased estimator is equal to the inverse of the Fisher information matrix. Considering an *unbiased* estimate $\widehat{\mathbf{p}}$ of $\mathbf{p}$ the Cramer-Rao bound states that

$$E\left[(\widehat{\mathbf{p}} - \mathbf{p})(\widehat{\mathbf{p}} - \mathbf{p})^T\right] \geq \mathcal{I}^{-1}(\mathbf{p}) \triangleq \mathcal{C}(\mathbf{p}) \tag{2}$$

where $\mathcal{I}(\mathbf{p})$ is the Fisher information matrix. In general, if $\mathcal{I}(\mathbf{p})$ is singular then no unbiased estimator for $\mathbf{p}$ exists with a finite variance [14], [15]. If $\mathcal{I}(\mathbf{p})$ is nonsingular then the existence of an unbiased estimator of $\mathbf{p}$ with finite variance is theoretically possible. If (2) holds with equality then the estimator is called *efficient* and the parameter estimate $\widehat{\mathbf{p}}$ is unique [15]. Finally, the condition (2) says nothing about the performance and realizability of biased estimators.

Consider the set of measurements from N sensors $\widehat{\mathbf{\Phi}} \sim \mathcal{N}(\mathbf{\Phi}(\mathbf{p}), \mathbf{R}_\phi)$. The Fisher information matrix in this case quantifies the amount of information that the observable random vector $\widehat{\mathbf{\Phi}}$ carries about the unobservable parameter $\mathbf{p}$. It is a matrix with the $(i,j)^{th}$ element given by

$$\left(\mathcal{I}\left(\mathbf{p}\right)\right)_{i,j} = E\left[\frac{\partial}{\partial \mathbf{p}_i} \ln\left(f_{\widehat{\mathbf{\Phi}}}(\widehat{\mathbf{\Phi}}; \mathbf{p})\right) \frac{\partial}{\partial \mathbf{p}_j} \ln\left(f_{\widehat{\mathbf{\Phi}}}(\widehat{\mathbf{\Phi}}; \mathbf{p})\right)\right]$$

where $\mathbf{p}_i$ is the i^{th} element of the target's location vector $\mathbf{p}$ (e.g. $\mathbf{p}_1 = x_p$ and $\mathbf{p}_2 = y_p$). Also, $f_{\widehat{\mathbf{\Phi}}}(\widehat{\mathbf{\Phi}}; \mathbf{p})$ is the likelihood function of $\mathbf{p}$ given fixed measurements and the natural logarithm of $f_{\widehat{\mathbf{\Phi}}}(\widehat{\mathbf{\Phi}}; \mathbf{p})$ is given by

$$\ln\left(f_{\widehat{\mathbf{\Phi}}}(\widehat{\mathbf{\Phi}}; \mathbf{p})\right) = \frac{1}{2}(\widehat{\mathbf{\Phi}} - \mathbf{\Phi}(\mathbf{p}))^{\mathrm{T}} \mathbf{R}_\phi^{-1} (\widehat{\mathbf{\Phi}} - \mathbf{\Phi}(\mathbf{p})) + c$$

where c is a constant term independent of $\mathbf{p}$. The general Fisher information matrix is then given by

$$\mathcal{I}(\mathbf{p}) = \nabla_{\mathbf{p}} \mathbf{\Phi}(\mathbf{p})^{\mathrm{T}} \mathbf{R}_\phi^{-1} \nabla_{\mathbf{p}} \mathbf{\Phi}(\mathbf{p}) \tag{3}$$

For the case of a single sensor measuring the bearing $\widehat{\phi}_1 = \phi_1(\mathbf{p}) + e_1$, the Fisher information matrix is given by

$$\mathcal{I}\left(\mathbf{p}\right) = \frac{1}{\sigma_e^2 r_i^2} \begin{bmatrix} \cos^2\left(\phi_1(\mathbf{p})\right) & -\frac{\sin(2\phi_1(\mathbf{p}))}{2} \\ -\frac{\sin(2\phi_1(\mathbf{p}))}{2} & \sin^2\left(\phi_1(\mathbf{p})\right) \end{bmatrix} \tag{4}$$

where $r_i = \|\mathbf{p} - \mathbf{s}_i\|$. Some simple calculations show that $\det|\mathcal{I}(\mathbf{p})| = \cos^2(\phi)\sin^2(\phi) - \frac{\sin^2(2\phi)}{4} \equiv 0$ is identically satisfied for any $\mathbf{p}$, and hence, unsurprisingly of course, no unbiased estimator with finite variance exists for the target location $\mathbf{p}$ with $N = 1$ bearing sensors.

The variance of the sum of independent random variables is equal to the sum of the variances. This immediately implies that the general Fisher information matrix for N bearing measurements is simply given by

$$\mathcal{I}\left(\mathbf{p}\right) = \frac{1}{\sigma_e^2} \sum_{i=1}^{N} \frac{1}{r_i^2} \begin{bmatrix} \cos^2\left(\phi_i(\mathbf{p})\right) & -\frac{\sin(2\phi_i(\mathbf{p}))}{2} \\ -\frac{\sin(2\phi_i(\mathbf{p}))}{2} & \sin^2\left(\phi_i(\mathbf{p})\right) \end{bmatrix} \tag{5}$$

where i indexes the bearing measurement from the i^{th} sensor. Independent measurements from additional sensors in general positions cannot decrease the total information.

Note that $\det\left(\mathcal{I}(\mathbf{p})\right)$ is inversely proportional to the uncertainty area of an unbiased estimate of $\mathbf{p}$ [15]. We use $\det\left(\mathcal{I}(\mathbf{p})\right)$ to analyze the sensor-emitter geometry and establish which sensor configurations minimize the variance (or mean-square-error) achievable by an efficient estimator.

In this paper we are not constructing estimators but rather characterizing the effect of the localization geometry on the performance of a generic unbiased and efficient estimator. In practice this analysis can only serve as a guide for sensor placement with biased estimation algorithms. Indeed, the relationship between the analysis conducted in this paper (assuming efficient unbiased estimators) and its applicability for biased estimators is yet to be completely understood. However, the goal of many localization algorithms, e.g. see [1], [2], is to obtain unbiased estimates (despite the fact that biased estimators have the ability to outperform the Cramer-Rao bound in terms of the mean square error achieved). Indeed, many localization algorithms attempt to remove the bias via additional processing [2]. Therefore, the results obtained in this paper are still of practical significance. In part 2 [6] we discuss the issue of biasedness in further detail.

The following result gives a means to approach the determinant maximization problem.

Theorem 1: Let $r_i = \|\mathbf{p} - \mathbf{s}_i\|$ be arbitrary but fixed for all $i \in \{1, \dots, N\}$. The following are equivalent expressions for the Fisher information determinant for bearing-only localization:

$$\text{(i)} \quad \det\left(\mathcal{I}\left(\mathbf{p}\right)\right) = \frac{1}{\sigma_\phi^4} \sum_{\mathcal{S}} \frac{\sin^2(\phi_j - \phi_i)}{r_i^2 r_j^2}, \quad j > i \tag{6}$$

$$\text{(ii)} \quad \det\left(\mathcal{I}\left(\mathbf{p}\right)\right) = \frac{1}{4\sigma_\phi^4} \left[\left(\sum_{i=0}^{N} \frac{1}{r_i^2}\right)^2 - \left(\sum_{i=0}^{N} \frac{\cos\left(2\phi_i\right)}{r_i^2}\right)^2 - \left(\sum_{i=0}^{N} \frac{\sin\left(2\phi_i\right)}{r_i^2}\right)^2\right] \tag{7}$$

where we define $\mathcal{S} = \{\{i, j\}\}$ to be the set of all combinations of i and j with $i, j \in \{1, \dots, N\}$ and $j > i$, implying that we have $|\mathcal{S}| = \binom{N}{2}$.

Proof: Note that $\mathbf{R}_\phi = \sigma_\phi^2 \mathbf{I}$ and thus $\mathbf{R}_\phi^{-1} = 1/\sigma_\phi^2 \mathbf{I}$. Let $\mathbf{G} = \nabla_{\mathbf{x}} \mathbf{y}(\mathbf{x})$ so that from (3) we also find

$$\det\left(\mathcal{I}\left(\mathbf{p}\right)\right) = \frac{1}{\sigma_\phi^4} \det\left(\mathbf{G}^{\mathrm{T}}\mathbf{G}\right) = \frac{1}{\sigma_\phi^4} \sum_{m=\{1,\ldots,\binom{N}{2}\}} \det\left(\mathbf{G}_m\right)^2$$

using the Cauchy-Binet formula, see e.g. [16]. Here $\mathbf{G}_m$ is a 2×2 minor of $\mathbf{G}$ taken from the set of minors indexed by $\mathcal{S} = \{\{i, j\}\}$. All 2×2 minors of $\mathbf{G}$ can be given as

$$\mathbf{G}_{\mathcal{S}} = \begin{bmatrix} \frac{1}{r_i}\cos(\phi_i) & \frac{1}{r_i}\sin(\phi_i) \\ \frac{1}{r_j}\cos(\phi_j) & \frac{1}{r_j}\sin(\phi_j) \end{bmatrix}$$

where in fact $\mathcal{S} = \{\{i, j\}\}$ with $|\mathcal{S}| = \binom{N}{2}$ can be considered the set of all combinations of i and j with $j > i$. Now the expression for the determinant given by (i) follows easily by trigonometry. For part (ii) we easily find that (5) can be rewritten as

$$\mathcal{I}\left(\mathbf{x}\right) = \frac{1}{\sigma_\phi^2} \begin{bmatrix} \sum_{i=0}^{N} \frac{(1+\cos(2\phi_i))}{2r_i^2} & -\sum_{i=0}^{N} \frac{\sin(2\phi_i)}{2r_i^2} \\ -\sum_{i=0}^{N} \frac{\sin(2\phi_i)}{2r_i^2} & \sum_{i=0}^{N} \frac{(1-\cos(2\phi_i))}{2r_i^2} \end{bmatrix}$$

Taking the determinant of this matrix and rearranging leads easily to (ii), see also [17]. ■

Any sensor-emitter configuration that maximizes the determinant in Theorem 1 is called an optimal sensor configuration and we will phrase sensor configurations in terms of the angles subtended at the emitter by the sensor-pairs given by $\vartheta_{ij} = \vartheta_{ji} \in [0, \pi)$. Again, we define optimality in the sense of minimizing the Cramer-Rao bound. Thus an unbiased and efficient estimator (if it exists) will achieve the smallest mean square error when the sensors are placed in an optimal configuration.

Corollary 1: Reflecting a sensor about the emitter position, i.e. moving a sensor from $\mathbf{s}_i$ *to* $2\mathbf{p} - \mathbf{s}_i$*, does not affect the value of the Fisher information determinant.*

Proof: Substituting $2\mathbf{p} - \mathbf{s}_i$ for $\mathbf{s}_i$ in the determinant given in Theorem 1 part (i) does not affect $r_i = \|\mathbf{p} - \mathbf{s}_i\|$ or $\sin^2(\phi_j - \phi_i)$ for any j. ■

Therefore, an optimal sensor configuration is not generally unique for given arbitrary sensor-emitter ranges.

The maximization of $\det\left(\mathcal{I}\left(\mathbf{p}\right)\right)$ can be solved on-the-fly in practice and it can be used to derive control laws for mobile sensors, i.e. gradient ascent based control laws are commonly employed, e.g. [18]. Subsequently, our focus is on explicitly analyzing the relative geometry in order to provide practitioners with some useful results upon which judgments can be made regarding the potential localization accuracy.

In the next section we examine a number of specific results regarding geometrical characterizations of bearing-only localization performance bounds.

4. On The Geometry of Bearing-Only Based Localization

In this section we characterize geometrical aspects of the bearings-only localization problem. The angle subtended at the target by two sensors i and j is $\vartheta_{ij} = \vartheta_{ji} \in [0, \pi)$.

A. The Optimal Geometry For Two Sensors and One Target

Here we characterize the geometry for two bearing sensors and one target. The main result of this subsection is now given.

Proposition 1: Given arbitrary ranges r_1 *and* r_2 *then the optimal two-sensor angular geometric arrangement for localization of a single target is when the angle* $\vartheta_{12} = \frac{\pi}{2}$.

Proof: From Theorem 1 part (i) we obtain the following optimization problem

$$\underset{\phi_1,\phi_2}{\operatorname{argmax}} \quad \frac{1}{r_1^2 r_2^2} \sin^2\left(\phi_2(\mathbf{p}) - \phi_1(\mathbf{p})\right)$$

which is solved when $\phi_2(\mathbf{p}) - \phi_1(\mathbf{p}) = c\frac{\pi}{2}$ where $c \in \pm\{1, 3\}$. This immediately implies that $\vartheta_{12} \equiv c\frac{\pi}{2} (\mathrm{mod}\ \pi) = \frac{\pi}{2}$. ■

The following result is also useful for geometric characterization of unbiased localization algorithms.

Proposition 2: No unbiased estimator of the target location $\mathbf{p}$ *exists with a finite variance when* $\tan(\phi_1(\mathbf{p})) = \tan(\phi_2(\mathbf{p}))$*, i.e. the two sensors are collinear with the target, or when* $r_1 \to \infty$ *or* $r_2 \to \infty$.

Proof: No unbiased estimator exists when the Fisher information matrix is singular which occurs when

$$\cos\left(\phi_1(\mathbf{p})\right)\sin\left(\phi_2(\mathbf{p})\right) - \cos\left(\phi_2(\mathbf{p})\right)\sin\left(\phi_1(\mathbf{p})\right) = 0$$

which implies $\tan(\phi_1(\mathbf{p})) = \tan(\phi_2(\mathbf{p}))$. The first part of the proposition is proved. If either r_1 or r_2 approach ∞ then $\frac{1}{r_1^2 r_2^2}$ approaches 0 and the Fisher information matrix is again singular. The proof of the proposition is complete. ■

We can observe the determinant value over a range of possible target locations and with a fixed sensor geometry. The sensor locations are given by $\mathbf{s}_1 = [-1/2\ 0]^T$ and $\mathbf{s}_2 = [1/2\ 0]^T$ and we plot the determinant value for target coordinates obeying $x_p \in [-3/2, 3/2]$ and $y_p \in [-3/2, 3/2]$. The illustration is given in Figure 1[1].

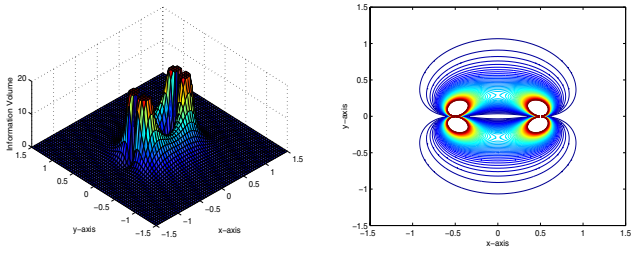

Fig. 1: The volume of the information ellipse for two sensors measuring the bearings to a target.

Observe in Figure 1 that the optimal geometries are clearly visible. Notably, given arbitrary ranges then the optimal geometry results in the target lying on the depicted semi-circular arcs which result in the angle subtended at the target by the two sensors being equal to $\frac{\pi}{2}$. Further, note that no unbiased (or biased [1]) estimator exists for target locations on the x-axis where the target would be collinear with both sensors.

[1]Note that as either target range, r_1 or r_2, approaches zero then the information volume approaches infinity. Hence, we limit the maximum volume displayed in the figure to 20. This explains the rings in the contour plot around the sensor positions and the flat peaks in the corresponding surface plot.

B. The Optimal Geometry For Three Sensors and One Target

The optimal localization geometry for three sensors and one target is described in this subsection. The main result of this subsection is given in the following theorem.

Theorem 2: Let r_i be arbitrary but fixed $\forall i \in \{1,2,3\}$. The optimal sensor configuration is not unique. Every optimal angular separation ϑ_{12}, ϑ_{13} and ϑ_{23} can be obtained by first solving

$$\begin{array}{rcl} \vartheta_{12} & = & \frac{1}{2}\arccos\left(\frac{r_2^4r_1^4-r_3^4r_1^4-r_3^4r_2^4}{2r_3^4r_2^2r_1^2}\right) \\ \vartheta_{13} & = & \frac{1}{2}\arccos\left(\frac{r_3^4r_1^4-r_3^4r_2^4-r_2^4r_1^4}{2r_3^2r_2^4r_1^2}\right) \\ \vartheta_{23} & = & \pi-\vartheta_{12}-\vartheta_{13} \end{array} \quad (8)$$

when the $\arccos(\cdot)$ *are defined to be real (which occurs simultaneously for ϑ_{12} and ϑ_{13}) and then by an application of Corollary 1. If no real solution for both ϑ_{12} and ϑ_{13} exists then* $\det\left(\mathcal{I}(\mathbf{x})\right)$ *is maximized when*

$$\begin{cases} \vartheta_{ij}=\frac{\pi}{2}, \text{ if } r_i<r_k \text{ or } r_j<r_k,\ i,j\in\{1,2,3\}/\{k\} \\ \vartheta_{ij}=0 \text{ or } \pi, \ \text{ otherwise} \end{cases} \quad (9)$$

where now (in the second solution (9)) we have automatically accounted for sensor reflections as per Corollary 1.

Proof: From Theorem 1 part (i) we can derive the following optimization problem

$$\underset{A,B}{\operatorname{argmax}}\ \alpha\sin^2(A)+\beta\sin^2(B)+\gamma\sin^2(B-A) \quad (10)$$

where $A=(\phi_2-\phi_1)$, $B=(\phi_3-\phi_1)$ and where $\alpha=r_3^2$, $\beta=r_2^2$ and $\gamma=r_1^2$ are arbitrary constants. Equating the gradient to zero and rearranging gives

$$\begin{array}{rcll} \alpha\sin(2A)+\beta\sin(2B) & = & 0 & (11) \\ \sin(2A)\left[\frac{\alpha}{\gamma}+\frac{\alpha}{\beta}\cos(2A)+\cos(2B)\right] & = & 0 & (12) \\ \sin(2B)\left[\frac{\beta}{\gamma}+\frac{\beta}{\alpha}\cos(2B)+\cos(2A)\right] & = & 0 & (13) \end{array}$$

From (11) we note that if $\sin(2A)=0$ then $\sin(2B)=0$ or if $\sin(2A)\neq 0$ then $\sin(2B)\neq 0$. Thus, $\sin(2A)=0$ and $\sin(2B)=0$ implies $A=\frac{c_A\pi}{2}$ and $B=\frac{c_B\pi}{2}$ with $c_A,c_B\in\mathbb{N}$. Also, if $\sin(2A)\neq 0\neq\sin(2B)$ then (12) and (13) lead to

$$\begin{array}{rcl} \left[\frac{\alpha}{\gamma}+\frac{\alpha}{\beta}\cos(2A)+\cos(2B)\right] & = & 0 \\ \left[\frac{\beta}{\gamma}+\frac{\beta}{\alpha}\cos(2B)+\cos(2A)\right] & = & 0 \end{array}$$

which can be solved for A and B to give

$$\begin{array}{rcll} A & = & \frac{1}{2}\arccos\left(\frac{\beta^2\gamma^2-\alpha^2\gamma^2-\alpha^2\beta^2}{2\alpha^2\beta\gamma}\right) & (14) \\ B & = & \frac{1}{2}\arccos\left(\frac{\alpha^2\gamma^2-\alpha^2\beta^2-\beta^2\gamma^2}{2\alpha\beta^2\gamma}\right) & (15) \end{array}$$

where the $\arccos(\cdot)$ are simultaneously real and hence A and B are defined by (14) and (15) appropriately only when the two respective conditions

$$\begin{array}{rcll} \left|\frac{\beta^2\gamma^2-\alpha^2\gamma^2-\alpha^2\beta^2}{2\alpha^2\beta\gamma}\right| & \leq & 1 & (16) \\ \left|\frac{\alpha^2\gamma^2-\alpha^2\beta^2-\beta^2\gamma^2}{2\alpha\beta^2\gamma}\right| & \leq & 1 & (17) \end{array}$$

are satisfied. Therefore, we now have two mutually exclusive sets of critical points corresponding to when $\sin(2A)=\sin(2B)=0$ and $\sin(2A)\neq 0\neq\sin(2B)$ respectively. If $A=\frac{c_A\pi}{2}$ and $B=\frac{c_B\pi}{2}$ then $\cos(2A)=\pm 1$ and $\cos(2B)=\pm 1$ which lie on the boundary of where (16) and (17) are satisfied. The maximizing values for A and B in (10) must change continuously for continuous changes in α, β and γ. The values for A and B given by (14) and (15) only connect smoothly with those found by solving $\sin(2A)=0$ and $\sin(2B)=0$ on the boundaries of where (16) and (17) are satisfied.

Therefore, if $A=\frac{c_A\pi}{2}$ and $B=\frac{c_B\pi}{2}$ solve (10) then they do so for all α, β and γ or they do so only when no real solutions exist via (14) and (15). Now it can be verified that if $\alpha=\beta=\gamma$ then both (16) and (16) are satisfied with strict inequality. Moreover, (14) and (15) give real solutions for A and B which lead to a greater value of (10) when compared to $A=\frac{c_A\pi}{2}$ and $B=\frac{c_B\pi}{2}$.

Hence, it follows that (14) and (15) maximize (10) when the conditions (16) and (17) are satisfied. Otherwise, the maximizing solutions of (10) are $A=\frac{c_A\pi}{2}$ and $B=\frac{c_B\pi}{2}$ with $c_A,c_B\in\mathbb{N}$. It is straightforward to find the relationship between the ϑ_{ij} and A and B when (14) and (15) give real solutions under the convention that $\phi_j\geq\phi_i$ when $j>i$ and $\forall i,j\in\{1,\ldots,N\}$.

When $A=\frac{c_A\pi}{2}$ and $B=\frac{c_B\pi}{2}$ maximize (10), then one of the $\sin^2(\cdot)$ terms in (10) is always zero while the other two $\sin^2(\cdot)$ terms are one. If $r_i<r_j$ and $r_i<r_k$, for $i,j,k\in\{1,2,3\}$ for $i\neq j\neq k$ then the $\sin^2(\cdot)$ term in (10) with r_i as a coefficient is the one that should be zero in order to solve the problem (10). With the substitution of $\alpha=r_3^2$, $\beta=r_2^2$, $\gamma=r_1^2$ we thus find that the proof is complete. ■

In general if the optimal geometry is given (originally) by (8) then Corollary 1 implies a maximum of four different optimal configurations can be obtained from the original solution (8) by reflecting sensors about the emitter. The following are two important special cases.

Corollary 2: When $r_1=r_2=r_3$ then a particular optimal geometry for bearing-only localization with three sensors and one target is when $\vartheta_{12}=\vartheta_{13}=\vartheta_{23}=\frac{2}{3}\pi$.

Corollary 3: When $r_1=r_2=r_3$ then a particular optimal geometry for bearing-only localization with three sensors and one target is when $\vartheta_{12}=\vartheta_{23}=\frac{1}{3}\pi$ and $\vartheta_{13}=\frac{2}{3}\pi$.

The following result characterizes a different aspect of the geometry for bearing-only localization with unbiased localization algorithms.

Proposition 3: No unbiased estimator of the target location $\mathbf{p}$ *exists with a finite variance when*

$$\tan(\phi_1(\mathbf{p}))=\tan(\phi_2(\mathbf{p}))=\tan(\phi_3(\mathbf{p}))$$

or when $r_i,r_j\to\infty$.

Proof: The proof involves determining when the Fisher information determinant is zero or when (10) is zero and hence the Fisher information matrix is singular. If we assume $r_i \neq 0$ and $r_i \neq \infty$ then each term becomes zero only when the following condition is satisfied

$$\cos(\phi_i(\mathbf{p}))\sin(\phi_j(\mathbf{p})) - \cos(\phi_j(\mathbf{p}))\sin(\phi_i(\mathbf{p})) = 0 \quad (18)$$

which implies $\tan(\phi_i(\mathbf{p})) = \tan(\phi_j(\mathbf{p}))$, $\forall, i, j \in \{1, 2, 3\}$. If two ranges r_i and r_j with $i \neq j$ approach ∞ then the determinant vanishes and the proof is complete. ■

The first condition in Proposition 3 implies that the three sensors are collinear with the target.

It is also clear that no biased estimator exists when the conditions of Proposition 3 hold.

Consider the following example which illustrates the change in optimal angular geometry in terms of the relative changes in sensor-target ranges. The illustration is given in Figure 2.

Figure 2 shows the variation of the optimal geometry as the range r_1 changes from $r_1 << r_2 = r_3$ to $r_1 >> r_2 = r_3$. The particular ranges and ϑ_{ij} (in degrees) are given in the figure titles. In Figure 2(a), the ranges are such that conditions (16) and (17) do not hold and hence the optimal geometry is such that sensor 1 forms right angles with sensors 2 and 3. At the other extreme in Figure 2(d), the ranges are such that $r_1 >> r_2 = r_3$ and hence sensor 2 and 3 are (almost) at right angles with sensor 1 splitting the major difference between sensors 2 and 3. From the theorem we find that as $r_1 \to \infty$ we expect $\vartheta_{23} \to \frac{\pi}{2}$ in this example. Sensor reflections over the emitter do not change the optimality of the geometry so this figure illustrates only the most intuitive examples.

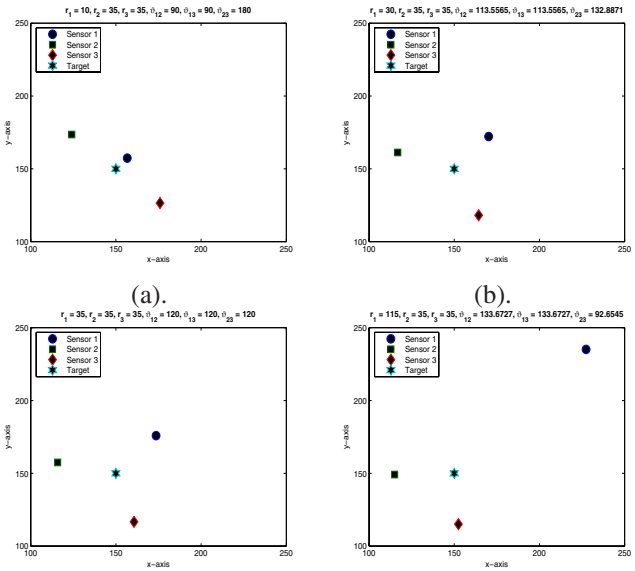

Fig. 2: This figure illustrates the different optimal sensor-target geometries for different ranges r_i from sensor i to the target. In this illustration, only r_1 changes from one graph to the next and the ranges and ϑ_{ij} (in degrees) are given in the figure titles. In part (a) the range $r_1 << r_2 = r_3$ means that the conditions (16) and (17) do not hold and hence the optimal relative sensor geometry shown is when $\vartheta_{12} = \vartheta_{13} = \frac{\pi}{2}$ and $\vartheta_{23} = \pi$ (or $\vartheta_{23} = 0$ is equivalently valid but not shown). In part (b) the range $r_1 < r_2 = r_3$ but the conditions (16) and (17) do hold and hence the optimal geometry is not a right angle geometry. In part (c) we see that when $r_1 = r_2 = r_3$ the optimal sensor geometry is equally spaced around the target. In part (d) we want to illustrate that as $r_1 >> r_2 = r_3$ the angle ϑ_{23} approaches $\frac{\pi}{2}$ as r_1 approaches ∞. Indeed, when $r_1 >> r_2 = r_3$, part (d) illustrates that we can easily approximate the optimal geometry as such. Recall from Corollary 1 that sensor reflections over the emitter do not change the optimality of the geometry and hence this figure illustrates only the most intuitive examples.

C. The Optimal Geometry for N Sensors and One Target

In this subsection we provide a number of important results concerning the optimal geometry for bearing-only localization with $N \geq 3$ sensors and one target. The case of $N = 2$ has been completely characterized and does not follow easily from the following discussion. Thus, in this section we generally assume $N \geq 3$.

Theorem 3: Given ranges $r_i = r_j, \forall i, j \in \{1, \ldots, N\}$ from each sensor to the target, the following statements hold true:

(i) *A point given by $(\phi_1, \ldots, \phi_N)$ is a critical point (i.e. a maximum, minimum or inflection) of the determinant given in Theorem 1 if*

$$\tan(2\phi_i(\mathbf{p})) = \tan(2\phi_j(\mathbf{p})) \quad (19)$$

for all $i, j \in \{1, \ldots, N\}$ or

$$\sum_{i=1}^{N} \sin(2\phi_i(\mathbf{p})) = 0 \text{ and } \sum_{i=1}^{N} \cos(2\phi_i(\mathbf{p})) = 0 \quad (20)$$

(ii) *The determinant vanishes if and only if $\tan(\phi_i(\mathbf{p})) = \tan(\phi_i(\mathbf{p}))$, $\forall i, j \in \{1, \ldots, N\}$. The determinant vanishes at the global minimum.*

(iii) *The solutions to (20) are globally maximizing values for the determinant given in Theorem 1.*

Proof: With no loss of generality let $r_i = r_j = 1$, $\forall i, j$ so that from Theorem 1 part (i) we obtain the optimization problem

$$\underset{\phi_1, \ldots, \phi_N}{\text{argmax}} \quad \sum_{\mathcal{S}} \sin^2(\phi_j - \phi_i) \quad (21)$$

where we define $\mathcal{S} = \{\{i, j\}\}$ to be the set of all combinations of i and j with $i, j \in \{1, \ldots, N\}$ and $j > i$, implying that $|\mathcal{S}| = \binom{N}{2}$. Taking the derivative of (21) with respect to ϕ_k, $\forall k \in \{1, \ldots, N\}$ leads to the following system of N equations

$$\frac{\partial}{\partial \phi_k} \sum_{\mathcal{S}} \sin^2(\phi_j - \phi_i) = \sum_{\substack{i=1 \\ i \neq k}}^{N} \sin(2(\phi_k - \phi_i)) =$$

$$\sin(2\phi_k) \sum_{i=1}^{N} \cos(2\phi_i) - \cos(2\phi_k) \sum_{i=1}^{N} \sin(2\phi_i) =$$

$$\begin{bmatrix} \sin(2\phi_k) & -\cos(2\phi_k) \end{bmatrix} \cdot \sum_{i=1}^{N} \begin{bmatrix} \cos(2\phi_i) \\ \sin(2\phi_i) \end{bmatrix} = 0$$

Noting that the summation is equivalent for all N equations with $k \in \{1, \ldots, N\}$, the gradient vanishes if and only if

$$\sum_{i=1}^{N} \sin(2\phi_i(\mathbf{p})) = 0 \text{ and } \sum_{i=1}^{N} \cos(2\phi_i(\mathbf{p})) = 0$$

or $\sum_{i=1}^{N}[\cos(2\phi_i)\ \sin(2\phi_i)]^{\mathrm{T}}$ is within the *null* space of $[\sin(2\phi_k)\ -\cos(2\phi_k)]$, $\forall k \in \{1,\ldots,N\}$. One particular scenario that satisfies the latter (*null* space) condition is when

$$\frac{\sin(2\phi_k)\cos(2\phi_i)-\cos(2\phi_k)\sin(2\phi_i)}{\|[\sin(2\phi_k)\ -\cos(2\phi_k)]\|\|[\sin(2\phi_i)\ \cos(2\phi_i)]^{\mathrm{T}}\|}=0$$

$\forall i,k \in \{1,\ldots,N\}$ which implies

$$\tan(2\phi_i)=\tan(2\phi_k),\quad \forall i,k\in\{1,\ldots,N\}$$

Thus, we have shown that the solutions to (19) and (20) are critical points of the optimization problem. This proves part (i) of Theorem 3. Part (ii) of Theorem 3 follows easily by inspection of (21) since each term of (21) must vanish. From Theorem 1 part (ii) with $r_i = 1, \forall i$ we find the determinant is upper-bounded by $\frac{N^2}{4\sigma_\phi^4}$ which is achievable if and only if (20) holds. This proves part(iii) of Theorem 3. ■

Remark 1: If $\phi_i = \phi_j \pm c_{ij}\pi/2, \forall i,j$ with $c_{ij} \in \{0,1,2,3\}$ then from (19) we know the determinant has a stationary point (e.g. minimum, maximum or inflection point). In general, the determinant will not vanish unless $c_{ij} \in \{0,2\}$, $\forall i,j$ which leads directly to part (ii) of Theorem 3. Furthermore, the determinant might or might not achieve the global upper-bound of $\frac{N^2}{4\sigma_\phi^4}$ depending on the number N of sensors and how many sensors are separated by $c\pi/2$ with $c \in \{1,3\}$.

Theorem 3 part (iii) implies the following useful corollary.

Proposition 4: Given ranges $r_i = r_j$, $\forall i,j \in \{1,\ldots,N\}$ from each sensor to the target, then the optimal sensor-target geometry is not unique when $N \geq 3$. Some particular optimal geometries for bearing-only localization with $N > 2$ sensors and one target can be obtained by first letting

$$\vartheta_{ij}=\vartheta_{ji}=\frac{2}{N}\pi,\quad \forall i,j\in\{1,\ldots,N\},\ \ j-i=1 \qquad (22)$$

or by letting

$$\vartheta_{ij}=\vartheta_{ji}=\frac{1}{N}\pi,\quad \forall i,j\in\{1,\ldots,N\},\ \ j-i=1 \qquad (23)$$

where $\vartheta_{ij} = \vartheta_{ji} \in [0,\pi)$ and then by an application of Corollary 1 on either (22) or (23). When $N = 2$ and $r_1 = r_2$, the unique optimal geometry occurs when $\vartheta_{12} = \vartheta_{21} = \frac{1}{2}\pi$.

Proof: The proof of this proposition is straightforward and involves verifying that the given (initial) conditions in the proposition satisfy part (iii) of Theorem 3. We omit the details for brevity. See also part 2 [6] of the pair of papers for a similar result for time-of-arrival based localization. ■

Proposition 4 implies the following corollary which summarizes the two intuitively appealing special cases.

Corollary 4: Assume that $r_i = r_j$, $\forall i,j \in \{1,\ldots,N\}$ and $\vartheta_{ij} = \vartheta_{ji} \in [0,\pi)$ with $j-i$ is the angle subtended at the target by two adjacent sensors i and j. Then $\vartheta_{ij} = \vartheta_{ji} = \frac{2}{N}\pi$ and $\vartheta_{ij} = \vartheta_{ji} = \frac{1}{N}\pi$ with $j-i=1$ and $\forall i,j \in \{1,\ldots,N\}$ are two separate optimal angular configurations of the N sensors relative to the single target.

Theorem 3 part (ii) implies the following useful corollary.

Corollary 5: Given that $r_i = r_j$, $\forall i,j \in \{1,\ldots,N\}$ then no unbiased estimator exists for the target location $\mathbf{p}$ when the condition of Theorem 3 part (ii) is satisfied.

Thus, we now have some intuitively appealing results on the bearing-only localization geometry for $N \geq 2$ sensors. In part 2 [6] we discuss further the practicality of the assumption of unbiased and efficient estimation which is inherent to the geometrical characterization in this paper [19], [20].

5. CONCLUSION

In this paper we explored the characteristics of the relative sensor-target geometry for bearing-only localization in $\mathbb{R}^2$. In particular, we illustrated via analysis that the optimal geometry can change significantly for sensors with non-equal target ranges. Indeed, we have shown that the assumption of uniform (angular) spacing is not even a good approximation when one of the sensors is much closer or much further away from the target relative to the other sensors. The analysis given in this paper is also related to optimal path planning and control of mobile sensors for localization, e.g. see [13], [18].

REFERENCES

[1] S.C. Nardone, A.G. Lindgren, and K.F. Gong. Fundamental properties and performance of conventional bearings-only target motion analysis. *IEEE Transactions on Automatic Control*, AC-29(9):775–787, 1984.

[2] M. Gavish and A.J. Weiss. Performance analysis of bearing-only target location algorithms. *IEEE Trans. Aero. Elect. Sys.*, 28(3):817–827, 1992.

[3] K. Dogancay. Bearings-only target localization using total least squares. *Signal Processing*, 85(9):1695–1710, Sept. 2005.

[4] K. Dogancay. Bias compensation for the bearings-only pseudolinear target track estimator. *IEEE Trans. Sig. Proc.*, 54(1):59–68, Jan. 2006.

[5] Special issue on time-delay estimation. *IEEE Transactions on Acoustic, Speech and Signal Processing*, ASSP-29, June 1981.

[6] A.N. Bishop, B. Fidan, B.D.O. Anderson, P.N. Pathirana, and K. Dogancay. Optimality analysis of sensor-target geometries in passive localization: Part 2 - Time-of-arrival based localization. In *ISSNIP'07*, Melbourne, Australia, December 2007.

[7] I. Kadar. Optimum geometry selection for sensor fusion. In *Proceedings of SPIE Conference on Signal Processing, Sensors Fusion and Target Recognition VII*, pages 96–107, Orlando, FL, 1998.

[8] A.G. Dempster. Dilution of precision in angle-of-arrival positioning systems. *Electronics Letters*, 42(5), March 2006.

[9] E. Fogel and M. Gavish. n^{th}-order dynamics target observability from angle measurements. *IEEE Transactions on Aerospace and Electronic Systems*, 24(3):305–308, 1988.

[10] K. Becker. Simple linear theory approach to TMA observability. *IEEE Trans. on Aero. and Elect. Sys.*, 29(2):575–578, 1993.

[11] C. Jauffret and D. Pillon. Observability in passive target motion analysis. *IEEE Trans. on Aero. and Elect. Sys.*, 32(4):1290–1300, Oct. 1996.

[12] T.L. Song. Observability of target tracking with bearings-only measurement. *IEEE Trans. on Aero. and Elect. Sys.*, 32(4):1468–1472, 1996.

[13] K. Dogancay. Optimized path planning for UAVs with AOA/scan based sensors. In 15^{th} *European Signal Processing Conference (EUSIPCO)*, Poznan, Poland, September 2007.

[14] P. Stoica and T.L. Marzetta. Parameter estimation problems with singular information matrices. *IEEE Trans. on Sig. Proc.*, 49(1):87–90, Jan. 2001.

[15] H.L. Van Trees. *Detection, Estimation and Modulation Theory*. John Wiley and Sons, Inc., New York, NY, 1968.

[16] R.A. Horn and C.R. Johnson. *Matrix Analysis*. Cambridge University Press, New York, NY, 1985.

[17] K. Dogancay and H. Hmam. Optimal angular sensor separation for AOA localization. (to be published).

[18] Y. Oshman and P. Davidson. Optimization of observer trajectories for bearings-only target localization. *IEEE Transactions on Aerospace and Electronic Systems*, 35(3):892–902, July 1999.

[19] Y.C. Eldar. Minimum variance in biased estimation: Bounds and asymptotically optimal estimators. *IEEE Transactions on Signal Processing*, 52(7):1915–1930, July 2004.

[20] Y.C. Eldar. Uniformly improving the Cramer-Rao bound and maximum-likelihood estimation. *IEEE Trans. Sig. Proc.*, 54(8):2943–2956, 2006.